Biosensors and Bioelectronics 52 (2014) 147–152

Contents lists available at ScienceDirect

Biosensors and Bioelectronics

journal homepage: www.elsevier.com/locate/bios

Direct electron transfer of glucose oxidase and biosensing for glucose based on PDDA-capped gold nanoparticle modified graphene/multi-walled carbon nanotubes electrode

Yanyan Yu [a], Zuanguang Chen [a,*], Sijing He [a], Beibei Zhang [a], Xinchun Li [b], Meicun Yao [a,*]

[a] School of Pharmaceutical Sciences, Sun Yat-sen University, Guangzhou 510006, China
[b] School of Pharmaceutical Sciences, Guangxi Medical University, Nanning 530021, China

ARTICLE INFO

Article history:
Received 28 June 2013
Received in revised form
17 August 2013
Accepted 20 August 2013
Available online 30 August 2013

Keywords:
Direct electron transfer
Gold nanoparticle
Multi-walled carbon nanotube
Graphene
Glucose oxidase
Biosensor

ABSTRACT

In this work, poly (diallyldimethylammonium chloride) (PDDA)-capped gold nanoparticles (AuNPs) functionalized graphene (G)/multi-walled carbon nanotubes (MWCNTs) nanocomposites were fabricated. Based on the electrostatic attraction, the G/MWCNTs hybrid material can be decorated with AuNPs uniformly and densely. The new hierarchical nanostructure can provide a larger surface area and a more favorable microenvironment for electron transfer. The AuNPs/G/MWCNTs nanocomposite was used as a novel immobilization platform for glucose oxidase (GOD). Direct electron transfer (DET) was achieved between GOD and the electrode. Field emission scanning electron microscopy (FESEM), UV–vis spectroscopy and cyclic voltammetry (CV) were used to characterize the electrochemical biosensor. The glucose biosensor fabricated based on GOD electrode modified with AuNPs/G/MWCNTs demonstrated satisfactory analytical performance with high sensitivity (29.72 mA M^{-1} cm^{-2}) and low limit of detection (4.8 μM). The heterogeneous electron transfer rate constant (K_S) and the apparent Michaelis–Menten constant (K_m) of GOD were calculated to be 11.18 s^{-1} and 2.09 mM, respectively. With satisfactory selectivity, reproducibility, and stability, the nanostructure we proposed offered an alternative for electrode fabricating and glucose biosensing.

1. Introduction

Graphene (G), a two-dimensional sheet of sp^2 bonded carbon atoms perfectly arranged in a honeycomb lattice (Novoselov et al., 2004), possesses high surface area, excellent electrical conductivity and high electrocatalytic activity. Due to its unique physicochemical properties (Huang et al., 2012), graphene has already demonstrated enormous potentials in a variety of fields. Whereas, graphene nanosheets are apt to aggregate after reduction, because of the strong van der Waals' and π–π interactions between individual sheets (Xu et al., 2008). As the 2D plane structure of graphene can provide a vast platform for loading various nanomaterials, graphene-based hybrid material has become a focus of research. Various nanoparticles have been reported to decorate graphene sheets, such as gold (Yang et al., 2011), silver (Liu et al., 2011a; Wang et al., 2011), platinum (Liu et al., 2011b), ferric oxide (Novoselov et al., 2004), and so on. Among them, gold nanoparticles (AuNPs) modified graphene has been extensively exploited as biosensors, as AuNPs can provide a suitable microenvironment to immobilize enzyme and facilitate the electron transfer between the immobilized enzyme and electrode surface (Chen et al., 2011; German et al., 2011; Ramanaviciene et al., 2009; Song et al., 2011; Wang et al., 2012). On the other hand, carbon nanotubes (CNTs), one of the carbon allotropes, have been investigated for more than two decades since its discovery (Iijima, 1991), owing to its unique electrical, thermal, and mechanic properties. Massive works have been done in terms of CNTs based electrochemical sensors and biosensors (Deng et al., 2009; Hu et al., 2011). It is worth mentioning that multi-walled carbon nanotubes (MWCNTs) have also been reported to form hybrid films with reduced graphene (Cai et al., 2008; Jang et al., 2012; Tung et al., 2009). The improvements in the physicochemical properties (conductivity, flexibility, and mechanical stability) of the G/MWCNTs composite are attributed to the distribution of graphene sheets in the MWCNTs bundles as well as the interfacial bonding between them. Many works have revealed that the G/MWCNTs composite films can be used to develop novel types of highly sensitive and stable electrochemical sensors (Huang et al., 2013; Woo et al., 2012; Zhang et al., 2011).

Glucose oxidase (GOD) is a flavin enzyme (Bankar et al., 2009), with molecular weight of 150–180 kDa, which has been widely used

* Corresponding authors. Tel.: +86 20 3994 3044; fax: +86 20 3994 3071.
E-mail addresses: chenzg@mail.sysu.edu.cn (Z. Chen), Lssymc@mail.sysu.edu.cn (M. Yao).

0956-5663/$ - see front matter © 2013 Elsevier B.V. All rights reserved.
http://dx.doi.org/10.1016/j.bios.2013.08.043

to monitor the blood glucose levels in diabetics (Kimmel et al., 2012). Since the concept of enzyme electrode was first introduced by Clark and Lyons (1962), GOD has been successively employed to fabricate glucose biosensors. The direct electron transfer (DET) between GOD and the electrode, however, is extremely difficult (Scognamiglio, 2013). As the active site of GOD, flavin adenine dinucleotide (FAD), is deeply embedded within a protective protein shell (Deng et al., 2008). Recently, great efforts have been made to improve DET between the redox-active sites of enzymes and the electrode surface, aiming to obtain a biosensor with better performances. A variety of materials, including quantum dots (Li et al., 2009; Liu et al., 2007b; Saa and Pavlov, 2012), molecular wire (Deng et al. 2007; Liu et al. 2007a), polymers (Li et al., 2012; Oztekin et al., 2011), metal or metal oxide nanoparticles (Patil et al., 2012; Zhao et al., 2006) and CNTs (Deng et al., 2010; Deng et al., 2008) have been used to modify the electrode for improving the DET. Especially, graphene and graphene-based hybrid materials are becoming a hot area of research, such as graphene quantum dots (Razmi and Mohammad-Rezaei, 2013), electrochemically reduced graphene (Liang et al., 2013; Unnikrishnan et al., 2013), G/chitosan (Kang et al., 2009; Liu et al., 2011a), G/PAMAM–silver nanoparticles/chitosan (Luo et al., 2012), G/CNTs/Nafion (Mani et al., 2013), and PVP/G/polyethylenimine (Shan et al., 2009).

In the present work, AuNPs modified G/MWCNTs hierarchical nanostructure was synthesized, for the first time, and was used to modify the electrode. Poly (diallyldimethylammonium chloride), PDDA, not only an electronic conducting polymer but also a strong ionic polymer, was utilized to synthesis PDDA-capped AuNPs. The positively charged AuNPs can be absorbed onto the negatively charged G/MWCNTs hybrid structure. Then GOD was immobilized onto the electrode through electrostatic attraction with AuNPs without any fixing materials (e.g. chitosan or Nafion). The graphene–nanotube–nanoparticle composite hierarchical structure provided a conductive network for efficient charge transfer as well as more binding sites for the enzyme. Satisfactory DET and accurate glucose determination were realized, indicating that the nanostructure we proposed could be an alternative for immobilizing biomolecules and fabricating biosensors.

2. Experimental

2.1. Chemicals and reagents

All chemicals were used as received unless otherwise stated. Graphite oxide and MWCNTs (ID: 5–12 nm, OD: 30–50 nm, length: 10–20 μm, –COOH: 0.73 wt%, purity: 95 wt%) were obtained from Nanjing XF NANO Materials Tech Co., Ltd (Nanjing China). Sodium phosphate monobasic, sodium phosphate dibasic, sodium hydroxide and hydrochloric acid were from Sinopharm reagent (Shanghai, China). Hydrazine hydrate, PDDA (MW=200,000–350,000, 20 wt% in water), glucose oxidase and glucose were from Aladin Chemistry Co. Ltd (Shanghai, China). Phosphate buffer solutions (PBS, 0.1 M) were prepared by mixing the stock solutions of 0.2 M NaH_2PO_4 and Na_2HPO_4. PBS (0.1 M) with pH from 3.0 to 8.0 was adjusted with hydrochloric acid or sodium hydroxide. All stock solutions were diluted with supporting electrolyte to the desired concentrations for analysis.

2.2. Apparatus and measurements

Cyclic voltammetry (CV) and chronoamperometry were performed on a CHI 810C electrochemical analyzer (Shanghai Chenhua instrument Co., Shanghai, China). A conventional three-electrode system was employed. An Ag/AgCl (saturated KCl) electrode and a platinum plate electrode were used as a reference electrode and a counter electrode, respectively. Bare or modified glassy carbon electrode (GCE) was used as a working electrode. All the electrochemical measurements were operated in ambient conditions. UV–vis absorption spectra were obtained using a UV2450 spectrophotometer (Shimadzu). Field emission scanning electron microscope (FESEM, JSM-6330 F) was used to characterize the morphology of the material.

2.3. Preparation of AuNPs/G/MWCNTs hybrid material

Graphene oxide (GO) aqueous dispersion was obtained from graphite oxide by sonication and centrifugation. GO/MWCNTs composites were prepared as reported by Woo et al. (2012) with a little modification. About 2.5 mg MWCNTs were added into 20 mL GO (0.5 mg mL^{-1}) aqueous dispersion and the solution was sonicated for 1 h. The obtained solution was then subjected to 30 min of centrifugation at 3000 rpm to remove extra MWCNTs.

PDDA-capped AuNPs with an average diameter of ~13 nm were prepared according to the reported literature (Chen et al., 2006). Typically, 50 μL PDDA (20 wt%), 20 mL water, 200 μL NaOH (0.5 M) and 100 μL $HAuCl_4$ (10 mg mL^{-1}) were added into a beaker. After being mixed thoroughly for 5 min, the solution was maintained at 100 °C for 20 min until the color of the solution changed to watermelon red.

To prepare the AuNPs/G/MWCNTs hybrid material, 6 mL GO/MWCNTs (0.5 mg mL^{-1}), 80 μL hydrazine hydrate (98 wt%), 20 μL PDDA (20 wt%), 6 mL PDDA-capped AuNPs were mixed. After sonication for 5 min, the dispersion was stirred for 30 min and was put in an oil bath at 100 °C equipped with a water-cooling condenser for 30 min to produce a homogeneous black suspension. The precipitate was collected by centrifugation and washed with water twice and then diluted by 6 mL water for electrode modification. To obtain the G/MWCNTs, the above procedure was adopted just in the absence of PDDA-capped AuNPs.

2.4. Fabrication of modified electrode

Prior to surface modification, GCE was polished with 0.05 μm-alumina slurries and sonicated with ethanol and deionized water, successively. After being dried with high purity nitrogen, the pretreated GCE was modified by dropping 5 μL of AuNPs/G/MWCNTs dispersion and dried at room temperature. Then the modified electrode was immersed into 0.1 M PBS (pH 7.0) containing 10 mg mL^{-1} GOD for 20 h at 4 °C. At this pH, GOD (pI ~ 4.5) bears net negative charge, and the modified electrode surface bares net positive charge. In this way, the GOD can be immobilized on the electrode surface through electrostatic attraction (Shan et al., 2009). The GOD/AuNPs/G/CNTs/GCE was rinsed carefully with double distilled water before use. For comparison, GOD/GCE, GOD/G/GCE and GOD/G/CNTs/GCE electrodes were also prepared in the same procedure. The enzyme-modified electrodes were stored at 4 °C when not in use. A schematic illustration of GOD immobilization was given in Scheme 1.

3. Results and discussion

3.1. Characterizations

The FESEM was utilized to characterize the morphology of the hybrid nanocomposite. As illustrated in Fig. 1A, long and tortuous MWCNTs and crumpled and rippled graphene have formed a homogeneous hybrid material, with some MWCNTs extruding from the wrapped structure, owing to the longer length of MWCNTs. The possible interaction was the π–π stacking interaction between the hydrophobic region of graphene and the sidewalls of MWCNTs

(Woo et al., 2012). When AuNPs were added, we can see from Fig. 1B that the G/MWCNTs hybrid material was decorated with a granular layer, AuNPs layer. Notably, the MWCNTs can also be uniformly decorated with AuNPs (Fig. 1C). As graphene and MWCNTs were negatively charged, the PDDA-capped AuNPs, which were positively charged, can be adsorbed onto the hybrid material (Xue et al., 2011), forming a hierarchical nanostructure with larger specific surface area and more binding sites for GOD.

UV–vis spectroscopy was utilized to monitor the reduction of GO and concomitant functionalization process. As shown in Fig. 1D, the UV–vis spectrum of GO dispersion exhibited a strong band at 229 nm, which was assigned to π–π transition. As for the GO/MWCNTs, the absorption peak red shifted to 236 nm, mainly due to the π–π stacking interaction between the aromatic basal plains of GO and MWCNTs (Mani et al., 2013). With regard to G/MWCNTs, the peak shifted to 264 nm, suggesting that the electronic conjugation within the graphene sheets was restored upon hydrazine reduction. Fig. 1E gave the UV–vis spectrum of gold colloids. There was characteristic surface plasmon absorption at 522 nm, typical for AuNPs of about 13 nm in diameter (Chen et al., 2006). And a color of watermelon red was presented by the colloids (inset).

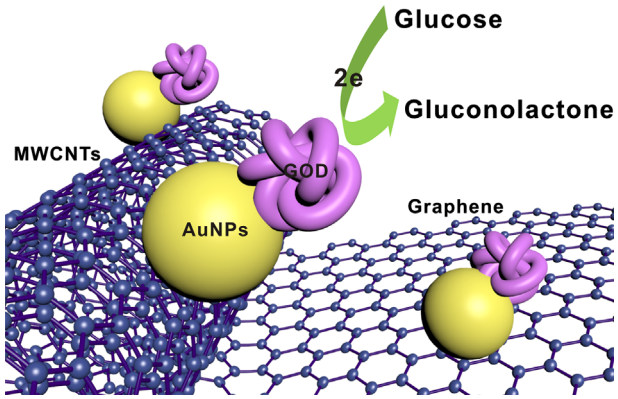

Scheme 1. Schematic illustration of construction of GOD/AuNPs/G/MWCNTs nanocomposites.

3.2. Direct electrochemistry of GOD immobilized in the AuNPs/G/MWCNTs film

Fig. 2 presented the cyclic voltammograms (CVs) for GOD (a), GOD/G (b) GOD/G/MWCNTs (c), GOD/AuNPs/G/MWCNTs (d) film modified GCE in 0.1 M PBS at a scan rate of 50 mV s^{-1}. No redox peaks were observed at GOD and GOD/G film modified GCE, indicating that DET of GOD was not achieved on these electrodes. Meanwhile, a pair of well-defined and quasi-reversible redox peaks was observed at both of the GOD/G/MWCNTs and GOD/AuNPs/G/MWCNTs modified electrode. On the contrary, no redox peak was observed on the electrodes modified with the same materials but without GOD (Fig. S1). Obviously, these redox peaks were characteristic of electron transfer process between redox active center (FAD) in the GOD and the electrode surface (Deng et al., 2008; Luo et al., 2012). Notably, the peak currents of curve (d), with formal potential ($E^{0'}$) of −0.4545 V and a peak-to-peak potential separation (ΔE_p) of 37 mV, were much higher than those of curve (c), demonstrating that the AuNPs/G/MWCNTs film was more beneficial to the direct electrochemistry of GOD than G/MWCNTs. The enhanced redox peak currents and low ΔE_p value indicated that a larger amount of GOD were immobilized and the interaction between the enzyme and the

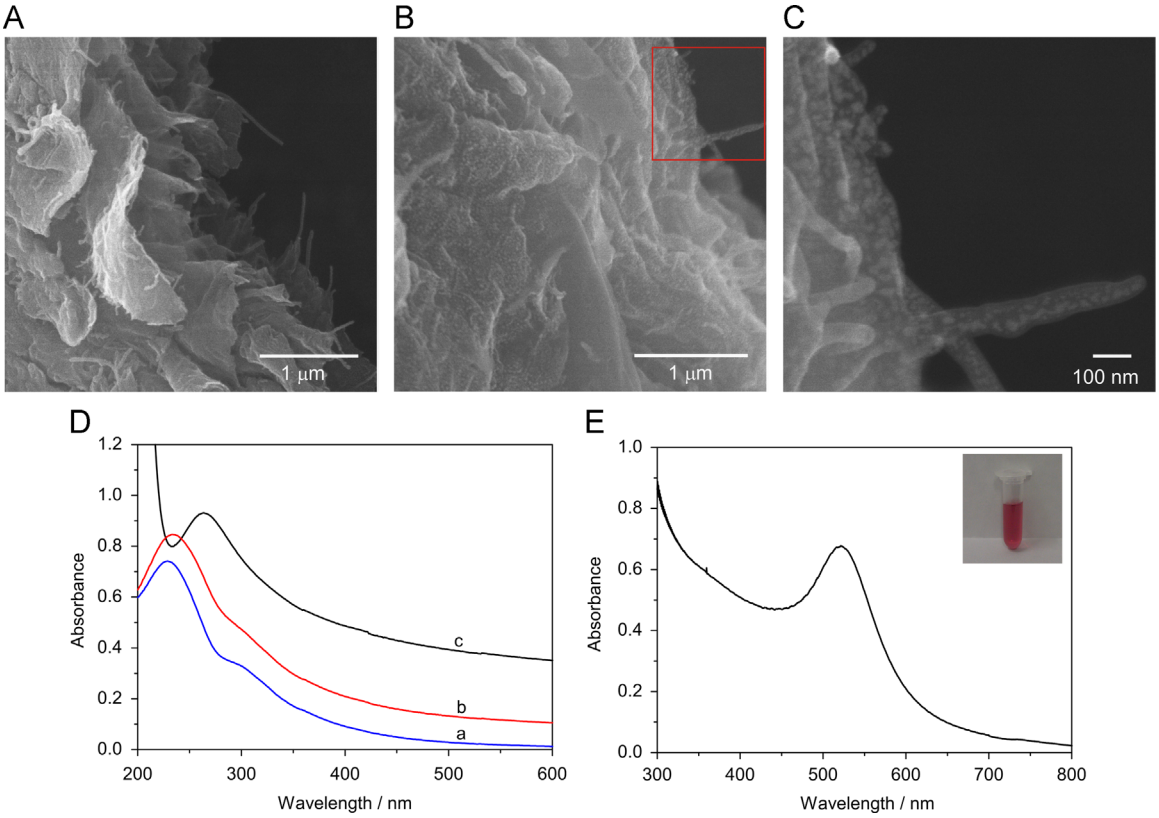

Fig. 1. (A) FESEM image of G/MWCNTs. (B) FESEM image of AuNPs/G/MWCNTs. (C) Magnified FESEM image of (B) marked in red box. (D) UV–vis absorption spectra of GO (a), GO–MWCNTs (b) and G–MWCNTs (c). (E) UV–vis absorption spectrum of PDDA-capped AuNPs. Inset: the photograph of PDDA-capped AuNPs. (For interpretation of the references to color in this figure caption, the reader is referred to the web version of this article.)

AuNPs/G/MWCNTs nanocomposite was more beneficial for electron transfer. The surface coverage (Γ) of GOD on the surface of AuNPs/G/MWCNTs modified electrode was calculated from the charge integration of cathodic peak of CVs at 50 mV s^{-1}. According to $\Gamma = Q/nFA$, where Q was the charge involved in the reaction, n was the number of electron transferred, F was Farady constant, and A was the geometric area of the electrode. Assume 2 for n, the value of Γ was calculated to be 2.22×10^{-10} M cm^{-2}, which was larger than that of GOD/CdTe/CNTs/Nafion modified electrode, 8.77×10^{-11} M cm^{-2} (Liu et al., 2007b), and the GOD/G/GCE, 1.22×10^{-10} M cm^{-2} (Unnikrishnan et al., 2013), indicating that the hybrid material we proposed was very beneficial for enzyme immobilization. This could be ascribed to the positive charges on the AuNPs containing film, which facilitated the immobilization of the enzyme.

3.3. Effect of scan rate and pH on the DET of GOD

Fig. 3A showed the effect of the scan rate on the CV performance at the GOD/AuNPs/G/MWCNTs/GCE in deoxygenated PBS (pH 7.0). The redox peak potentials of GOD shifted slightly with the increase of scan rate. The anodic peak current (I_{pa}) and cathodic peak current (I_{pc}) increased linearly with the increase of scan rate ranging from 50 to 1000 mV s^{-1} (inset I of Fig. 3A), suggesting that the redox reaction of GOD in AuNPs/G/MWCNTs/GCE was a quasi-reversible surface-controlled process (Shan et al., 2009). We can see from inset II of Fig. 3A that the anodic and cathodic peak potentials (E_{pa} and E_{pc}) were linearly dependent on the logarithm of the scan rates in the range of 500–1000 mV s^{-1}. With $2.3RT/(1-\alpha)nF$ and $-2.3RT/\alpha nF$ for the slops of the regression equations, respectively, the value of α (charge transfer coefficient) was calculated to be 0.57. According to the Laviron equation (Laviron, 1979), the electron transfer rate constant (K_S) can be calculated as follows:

$$\log K_S = \alpha \log(1-\alpha) + (1-\alpha)\log\alpha - \log(RT/nFv) - \alpha(1-\alpha)nF\Delta E_p/2.3RT \quad (1)$$

In Eq. (1), α represented the charge transfer coefficient (0.57), and all the other parameters represented their usual meanings. Taking the scan rate of 500 mV s^{-1}, K_S was calculated to be 11.18 s^{-1}, which was comparatively larger than those reported on G/CNTs/Nafion (3.02 s^{-1}) (Mani et al., 2013), G/PAMAM–silver nanoparticles/chitosan (8.59 s^{-1}), (Luo et al., 2012), graphene (4.8 s^{-1}) (Unnikrishnan et al., 2013), graphene quantum dots (1.12 s^{-1}) (Razmi and Mohammad-Rezaei, 2013), and MWCNTs–nanoflake-like SnS_2 nanocomposite (3.96 s^{-1}) (Li et al., 2013). The results confirmed that the GCE modified with AuNPs/G/MWCNTs nanocomposite enabled fast DET between the FAD and the surface of electrode.

The influence of pH value on the electrochemical behavior of GOD on the AuNPs/G/MWCNTs modified electrode was shown in Fig. 3B. As exhibited, both the cathodic and anodic peak potentials shift negatively with the increase of solution pH from 3.0 to 8.0. The plot of pH versus $E^{\theta'}$ (inset of Fig. 3B) exhibited a linear relationship over the entire pH range. The slope of linear regression equation was −51.2 mV pH^{-1}, which was in close agreement with the theoretical value of −58.5 mV pH^{-1} (Huang et al., 2005), proving participation of two protons ($2H^+$) and two electrons (2e) in the redox reaction.

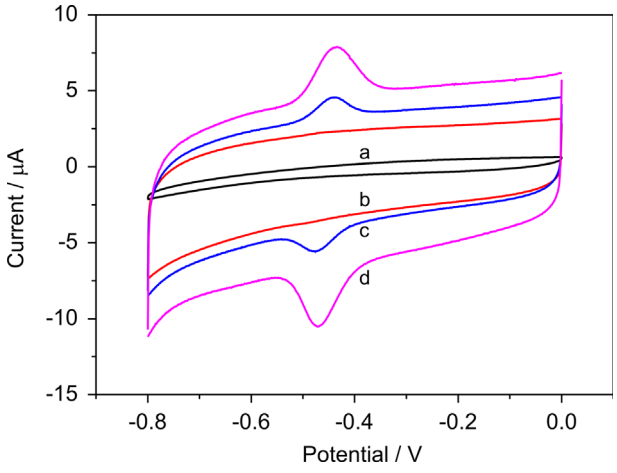

Fig. 2. CVs of GOD (a), GOD/G (b) GOD/G/MWCNTs (c), GOD/AuNPs/G/MWCNTs (d) film modified GCE in 0.1 M deoxygenated PBS at a scan rate of 50 mV s^{-1}.

3.4. Detection of glucose based on direct electrochemistry of GOD

Firstly, CV was utilized to characterize the electrochemical behavior of the modified electrodes. Fig. S2 exhibited that all the electrodes modified nonenzymatically had varying reduction peaks corresponding to the reduction of oxygen in air-saturated PBS. Notably, the AuNPs/G/MWCNTs hybrid material showed a great potential catalytic ability to oxygen reduction. In the case of AuNPs/G/MWCNTs/GCE, no obvious variation can be observed in the CVs upon addition of 2 mM glucose into the air-saturated PBS (Fig. S3), indicating that glucose did not make any influence to the redox reaction. As for the GOD/AuNPs/G/MWCNTs/GCE, however, the situation was quite different. We can see from Fig. 4 that the enzymatically modified electrode showed a significantly increased reduction peak current of FAD in air-saturated PBS (curve a), and the oxidation peak current of $FADH_2$ decreased meanwhile. The electrocatalytic process can be expressed as follows

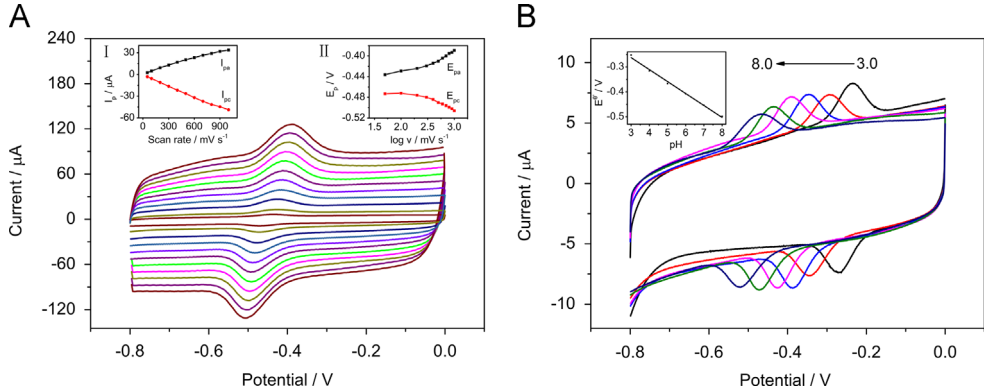

Fig. 3. (A) CVs of GOD/AuNPs/G/MWCNTs/GCE in 0.1 M deoxygenated PBS (pH 7.0) at different scan rates (from inner to outer: 50, 100, 200, 300, 400, 500, 600, 700, 800, 900 and 1000 mV s^{-1}). Inset: (I) linear dependence of I_{pa} and I_{pc} on scan rates. (II) linear dependence of E_{pa} and E_{pc} on logarithm of the scan rates. (B) CVs of GOD/AuNPs/G/MWCNTs/GCE in PBS with pH ranging from 3.0 to 8.0 at a scan rate of 50 mV s^{-1}. Inset: plot of pH versus $E^{\theta'}$.

(Liu and Ju, 2003):

$$GOD(FAD) + 2e^- + 2H^+ \leftrightharpoons GOD(FADH_2) \quad (2)$$

$$GOD(FADH_2) + O_2 \rightarrow GOD(FAD) + H_2O_2 \quad (3)$$

In this EC catalytic process (Bard and Faulkner, 2001), the oxidized form (FAD) was regenerated at the surface of the electrode and enhanced the reduction peak current of FAD in the presence of oxygen, which demonstrated that GOD efficiently catalyzed the oxygen reduction in this process. When glucose was added, the reduction peak current decreased (curve b). This can be explained that the enzyme-catalyzed reaction between GOD (FAD) and glucose diminished the concentration of the GOD (FAD), as shown in the following equation:

$$Glucose + GOD(FAD) \rightarrow gluconolactone + GOD(FADH_2) \quad (4)$$

Therefore, the electrode we fabricated was capable of detection glucose by monitoring the variation of the reduction currents.

Chronoamperometry was further used to illustrate the relationship between the electrocatalytic reduction current and the concentration of glucose. The amperometric response of GOD/AuNPs/G/MWCNTs/GCE at a constant potential of −0.45 V upon successive addition of glucose into air-saturated supporting electrolyte (0.1 M PBS, pH 7.0) was illustrated in Fig. 5 (A and B). The reduction currents achieved 95% of the steady-state current within 5 s and decreased with the successive addition of glucose over the wide concentration ranges 5–175 μM (Fig. 5A) and 0.3–2.1 mM (Fig. 5B).

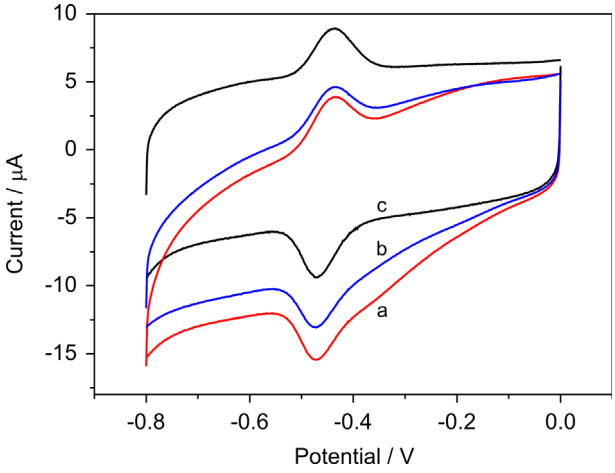

Fig. 4. CVs of GOD/AuNPs/G/MWCNTs/GCE in air-saturated PBS (a), air-saturated PBS including 2 mM glucose (b) and N_2-saturated PBS (c) at a scan rate of 50 mV s^{-1}.

As shown in the inset of Fig. 5A, the reduction steady-state currents decreased linearly with the concentration of glucose ranging from 5 to 175 μM. The linear regression equation was I (μA) = −6.4858 + 0.0021C (μM) with a correlation coefficient (r) of 0.9989. The limit of detection (LOD, S/N = 3) was 4.8 μM. The sensitivity was calculated to be 29.72 mA M^{-1} cm^{-2}. Fig. 5B illustrated the variation of reduction steady-state currents upon successive addition of 0.3 mM glucose into PBS. The electrode response showed a linear relationship from 0.3 to 2.1 mM, with I (μA) = −6.9642 + 1.40625C (mM) (r = 0.9938) for the linear regression equation. In the concentration range higher than 2.1 mM, the response deviated from linearity and leveled off, exhibiting a typical Michaelis–Menten kinetic mechanism. The apparent Michaelis–Menten constant (K_m) can be obtained from the Lineweaver–Burk equation as follows (Li et al. 1996):

$$1/I_{ss} = 1/I_{max} + K_m/I_{max}C \quad (5)$$

C was the concentration of glucose in solution, I_{ss} was the steady-state current (background current deducted), and I_{max} was the maximum current. K_m was calculated to be 2.09 mM according to the intercept and the slope of the plot of the reciprocals of I_{ss} vs. C. The low K_m verified that GOD maintained its native structure after immobilization in AuNPs/G/MWCNTs film, resulting in high affinity and activity towards glucose.

The comparison of analytical performances to those reported in the literatures concerning glucose biosensors was shown in Table S1. The results demonstrated that the GOD/AuNPs/G/MWCNTs/GCE was relatively sensitive, with a low LOD and K_m.

3.5. Reproducibility and stability of the modified electrode

The repeatability and reproducibility of the biosensor were evaluated by CV in PBS (0.1 M, pH 7.0) containing 0.5 mM glucose. The responses of six successive measurements gave a RSD of 4.1%, demonstrating a good repeatability. And five modified electrodes prepared independently showed a satisfied reproducibility with 5.3% for RSD.

With regard to stability, the CV responses remained 95% of the initial current after 20 cycles at a scan rate of 50 mV s^{-1}, proving the excellent stability of the fabricated electrode. After being stored for three weeks in 0.1 M pH 7.0 PBS at 4 °C, the biosensor still retains 89% of its original sensitivity. The good reproducibility and stability of the biosensor can be attributed to the strong interaction between enzyme and the electrode surface, confirming that the immobilization protocol we proposed not only retained the electrocatalytic activity of GOD, but also prevented it from falling off from the electrode surface.

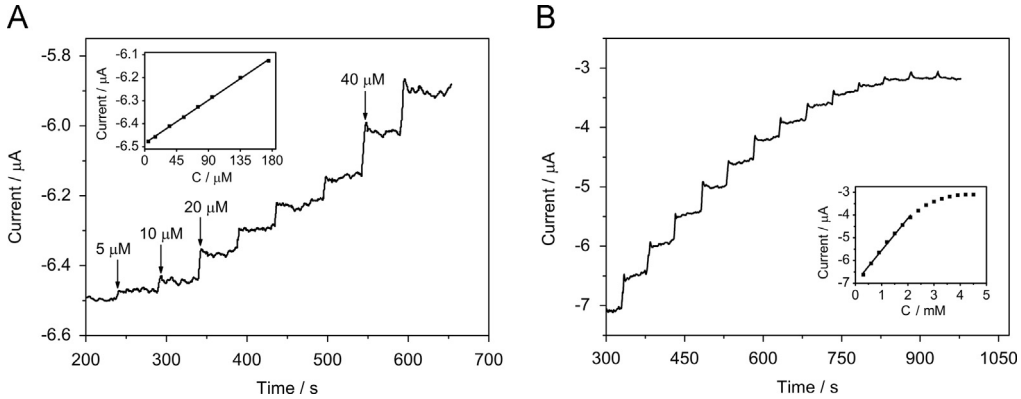

Fig. 5. (A) Amperometric response of GOD/AuNPs/G/MWCNTs/GCE at a constant potential of −0.45 V upon successive addition of glucose into 0.1 M PBS (pH 7.0). Inset: linear relationship of steady-state currents versus glucose concentrations. (B) Amperometric response of GOD/AuNPs/G/MWCNTs/GCE at a constant potential of −0.45 V upon successive addition of 0.3 mM glucose into 0.1 M PBS (pH 7.0). Inset: linear relationship of steady-state currents versus glucose concentrations.

3.6. Interference study and real sample analysis

It is known that dopamine, ascorbic acid (AA), uric acid (UA), which are easily oxidized, always coexist with glucose in human blood. Interference study was conducted under the optimal conditions for determination of glucose by the amperometric technique in the presence of 0.5 mM glucose. No obvious change in the glucose signal was observed when 0.5 mM of these substances were added to the electrolyte solution.

In order to investigate the practical application of the developed biosensor in clinical analysis, the GOD/AuNPs/G/MWCNTs modified electrode was utilized to detect glucose in human serum samples without any sample pretreatment except a dilution step (10-fold with PBS). The concentration of glucose in a serum sample was determined to be 4.85 mM, which was close to the value of 4.98 mM obtained by the spectrophotometry. The accuracy of the analytical method was evaluated by recovery test. Three different amounts of glucose were spiked and the recovery rate ranged from 93.3% to 104% ($n=3$), exhibiting a good accuracy for the determination of glucose in real samples. The results indicated that the method we developed was reliable and applicable in real human sample analysis.

4. Conclusions

In this study, AuNPs/G/MWCNTs nanocomposite was fabricated, which can immobilize GOD on the surface of the modified electrode through electrostatic interaction. DET was achieved between enzyme and the electrode with high electrocatalytic activities towards glucose, owing to the unique microenvironment of the nanocomposite. The glucose biosensor based on AuNPs/G/MWCNTs nanocomposite showed the satisfactory analytical performance. The sensitivity and LOD were 29.72 mA M^{-1} cm^{-2} and 4.8 μM, respectively. Interference from UA and AA was almost negligible to the glucose detection. The satisfactory performance of the glucose biosensor made it a qualified alternative for glucose determination in practical and routine analyses.

Acknowledgments

Financial supports from the National Natural Science Foundation of China (Nos. 20727006 and 21075139), the Fundamental Research Funds for the Central Universities, and Guangdong Provincial Science and Technology Project (No. 2008A030102009) are gratefully acknowledged.

Appendix A. Supplementary material

Supplementary data associated with this article can be found in the online version at http://dx.doi.org/10.1016/j.bios.2013.08.043.

References

Bankar, S.B., Bule, M.V., Singhal, R.S., Ananthanarayan, L., 2009. Biotechnology Advances 27 (4), 489–501.
Bard, A.J., Faulkner, L.R., 2001. Electrochemical Methods: Fundamentals and Applications, third ed. John Wiley & Sons, Inc., New York.
Cai, D.Y., Song, M., Xu, C.X., 2008. Advanced Materials 20 (9), 1706–1709.
Chen, H.J., Wang, Y.L., Wang, Y.Z., Dong, S.J., Wang, E.K., 2006. Polymer 47 (2), 763–766.
Chen, Y., Li, Y., Sun, D., Tian, D.B., Zhang, J.R., Zhu, J.J., 2011. Journal of Materials Chemistry 21 (21), 7604–7611.
Clark, L.C., Lyons, C., 1962. Annals of the New York Academy of Sciences 102, 29–45.
Deng, C.Y., Chen, J.H., Chen, X.L., Mao, C.H., Nie, L.H., Yao, S.Z., 2008. Biosensors and Bioelectronics 23 (8), 1272–1277.
Deng, C.Y., Chen, J.H., Nie, Z., Si, S.H., 2010. Biosensors and Bioelectronics 26 (1), 213–219.
Deng, L., Liu, Y., Yang, G.C., Shang, L., Wen, D., Wang, F., Xu, Z., Dong, S.J., 2007. Biomacromolecules 8 (7), 2063–2071.
Deng, S.Y., Jian, G.Q., Lei, J.P., Hu, Z., Ju, H.X., 2009. Biosensors and Bioelectronics 25 (2), 373–377.
German, N., Ramanavicius, A., Voronovic, J., Oztekin, Y., Ramanaviciene, A., 2011. Microchimica Acta 172 (1-2), 185–191.
Hu, F.X., Chen, S.H., Wang, C.Y., Yuan, R., Chai, Y.Q., Xiang, Y., Wang, C., 2011. Journal of Molecular Catalysis B: Enzymatic 72 (3–4), 298–304.
Huang, T.Y., Huang, J.H., Wei, H.Y., Ho, K.C., Chu, C.W., 2013. Biosensors and Bioelectronics 43, 173–179.
Huang, X., Qi, X.Y., Boey, F., Zhang, H., 2012. Chemical Society Reviews 41 (2), 666–686.
Huang, Y.X., Zhang, W.J., Xiao, H., Li, G.X., 2005. Biosensors and Bioelectronics 21 (5), 817–821.
Iijima, S., 1991. Nature 354, 56–58.
Jang, W.S., Chae, S.S., Lee, S.J., Song, K.M., Baik, H.K., 2012. Carbon 50 (3), 943–951.
Kang, X.H., Wang, J., Wu, H., Aksay, I.A., Liu, J., Lin, Y.H., 2009. Biosensors and Bioelectronics 25 (4), 901–905.
Kimmel, D.W., LeBlanc, G., Meschievitz, M.E., Cliffel, D.E., 2012. Analytical Chemistry 84 (2), 685–707.
Laviron, E., 1979. Journal of Electroanalytical Chemistry and Interfacial Electrochemistry 101 (1), 19–28.
Li, J., Tan, S.N., Ge, H., 1996. Analytica Chimica Acta 335 (1–2), 137–145.
Li, J., Yang, Z.J., Tang, Y., Zhang, Y.C., Hu, X.Y., 2013. Biosensors and Bioelectronics 41, 698–703.
Li, J.P., Li, Y.P., Zhang, Y., Wei, G., 2012. Analytical Chemistry 84 (4), 1888–1893.
Li, X.Y., Zhou, Y.L., Zheng, Z.Z., Yue, X.L., Dai, Z.F., Liu, S.Q., Tang, Z.Y., 2009. Langmuir 25 (11), 6580–6586.
Liang, B., Fang, L., Yang, G., Hu, Y.C., Guo, X.S., Ye, X.S., 2013. Biosensors and Bioelectronics 43, 131–136.
Liu, G.Z., Paddon-Row, M.N., Gooding, J.J., 2007a. Electrochemistry Communications 9 (9), 2218–2223.
Liu, Q., Lu, X.B., Li, J., Yao, X., Li, J.H., 2007b. Biosensors and Bioelectronics 22 (12), 3203–3209.
Liu, S., Tian, J.Q., Wang, L., Luo, Y.L., Lu, W.B., Sun, X.P., 2011a. Biosensors and Bioelectronics 26 (11), 4491–4496.
Liu, S., Tian, J.Q., Wang, L., Sun, X.P., 2011b. Carbon 49 (10), 3158–3164.
Liu, S.Q., Ju, H.X., 2003. Biosensors and Bioelectronics 19 (3), 177–183.
Luo, Z.M., Yuwen, L.H., Han, Y.J., Tian, J., Zhu, X.R., Weng, L.X., Wang, L.H., 2012. Biosensors and Bioelectronics 36 (1), 179–185.
Mani, V., Devadas, B., Chen, S.M., 2013. Biosensors and Bioelectronics 41, 309–315.
Novoselov, K.S., Geim, A.K., Morozov, S.V., Jiang, D., Zhang, Y., Dubonos, S.V., Grigorieva, I.V., Firsov, A.A., 2004. Science 306 (5696), 666–669.
Oztekin, Y., Ramanaviciene, A., Yazicigil, Z., Solak, A.O., Ramanavicius, A., 2011. Biosensors and Bioelectronics 26 (5), 2541–2546.
Patil, D., Dung, N.Q., Jung, H., Ahn, S.Y., Jang, D.M., Kim, D., 2012. Biosensors and Bioelectronics 31 (1), 176–181.
Ramanaviciene, A., Nastajute, G., Snitka, V., Kausaite, A., German, N., Barauskas-Memenas, D., Ramanavicius, A., 2009. Sensors and Actuators B: Chemical 137 (2), 483–489.
Razmi, H., Mohammad-Rezaei, R., 2013. Biosensors and Bioelectronics 41, 498–504.
Saa, L., Pavlov, V., 2012. Small 8 (22), 3449–3455.
Scognamiglio, V., 2013. Biosensors and Bioelectronics 47C, 12–25.
Shan, C.S., Yang, H.F., Song, J.F., Han, D.X., Ivaska, A., Niu, L., 2009. Analytical Chemistry 81 (6), 2378–2382.
Song, W., Li, D.W., Li, Y.T., Li, Y., Long, Y.T., 2011. Biosensors and Bioelectronics 26 (7), 3181–3186.
Tung, V.C., Chen, L.M., Allen, M.J., Wassei, J.K., Nelson, K., Kaner, R.B., Yang, Y., 2009. Nano Letters 9 (5), 1949–1955.
Unnikrishnan, B., Palanisamy, S., Chen, S.M., 2013. Biosensors and Bioelectronics 39 (1), 70–75.
Wang, Y., Yuan, R., Chai, Y.Q., Yuan, Y.L., Bai, L.J., 2012. Biosensors and Bioelectronics 38 (1), 50–54.
Wang, Y.L., Liu, L., Li, M.G., Xu, S.D., Gao, F., 2011. Biosensors and Bioelectronics 30 (1), 107–111.
Woo, S., Kim, Y.R., Chung, T.D., Piao, Y., Kim, H., 2012. Electrochimica Acta 59, 509–514.
Xu, Y.X., Bai, H., Lu, G.W., Li, C., Shi, G.Q., 2008. Journal of the American Chemical Society 130 (18), 5856–5857.
Xue, Y., Zhao, H., Wu, Z.J., Li, X.J., He, Y.J., Yuan, Z.B., 2011. Biosensors and Bioelectronics 29 (1), 102–108.
Yang, X., Xu, M.S., Qiu, W.M., Chen, X.Q., Deng, M., Zhang, J.L., Iwai, H., Watanabe, E., Chen, H.Z., 2011. Journal of Materials Chemistry 21 (22), 8096–8103.
Zhang, Y., Yuan, R., Chai, Y.Q., Li, W.J., Zhong, X., Zhong, H.A., 2011. Biosensors and Bioelectronics 26 (9), 3977–3980.
Zhao, S., Zhang, K., Bai, Y., Yang, W.W., Sun, C.Q., 2006. Bioelectrochemistry 69 (2), 158–163.